2007/12/13

Superconducting gap structure of Sr_2RuO_4 from a microscopic theory.

Takuji NOMURA
Synchrotron Radiation Research Unit
Japan Atomic Energy Agency

Collaborators:

Kosaku YAMADA
Prof. (Emeritus), Kyoto University

Hiroaki Ikeda
Kyoto University

Points of the talk

Full gap is expected on the Fermi surfaces in the chiral *p*-wave state
in general. But power-law temperature dependences
(i.e., line-node-like behaviors) are experimentally observed
in many quantities.

(Let's remember that this complication was mentioned
in the Blackboard Lunch Talk last Monday by Prof. Sigrist.)

How to reconcile ?

We propose a possible way by our microscopic theory.

- Analysis of *T* dependence of physical quantities:
  - Specific heat (Exp. data by Nishizaki, Deguchi, Maeno),
  - Sound attenuation rate (Exp. data by C. Lupien et al.),
  - Thermal conductivity (Exp. data by M. Tanatar et al.),
  - NMR relaxation rate (Exp. data by K. Ishida et al.).

2D three-band Hubbard model for Sr_2RuO_4 and Eliashberg equation

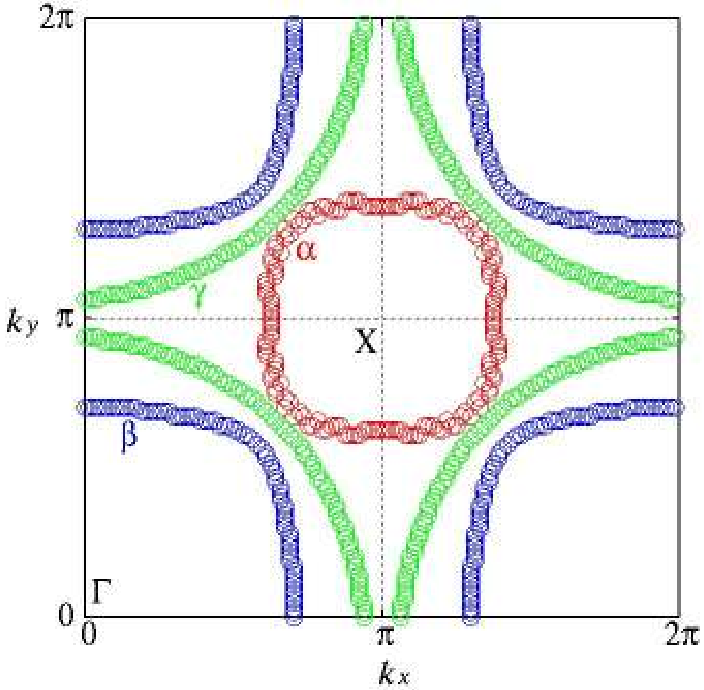

$$H = H_0 + H'$$

$$H_0 = -\sum_{\mathbf{x}\mathbf{x}'\ell\ell'\sigma} t_{\mathbf{x}\ell,\mathbf{x}'\ell'} c^{+}_{\mathbf{x}\ell\sigma} c_{\mathbf{x}'\ell'\sigma} \qquad \ell,\ell' = xy, yz, xz$$

$$H' = \frac{U}{2}\sum_{\mathbf{x}\ell\sigma\neq\sigma'} c^{+}_{\mathbf{x}\ell\sigma} c^{+}_{\mathbf{x}\ell\sigma'} c_{\mathbf{x}\ell\sigma'} c_{\mathbf{x}\ell\sigma} + \frac{U'}{2}\sum_{\mathbf{x}\ell\neq\ell'\sigma\sigma'} c^{+}_{\mathbf{x}\ell\sigma} c^{+}_{\mathbf{x}\ell'\sigma'} c_{\mathbf{x}\ell'\sigma'} c_{\mathbf{x}\ell\sigma}$$

$$+ \frac{J}{2}\sum_{\mathbf{x}\ell\neq\ell'\sigma\sigma'} c^{+}_{\mathbf{x}\ell\sigma} c^{+}_{\mathbf{x}\ell'\sigma'} c_{\mathbf{x}\ell\sigma'} c_{\mathbf{x}\ell'\sigma} + \frac{J'}{2}\sum_{\mathbf{x}\ell\neq\ell'\sigma\neq\sigma'} c^{+}_{\mathbf{x}\ell\sigma} c^{+}_{\mathbf{x}\ell\sigma'} c_{\mathbf{x}\ell'\sigma'} c_{\mathbf{x}\ell'\sigma}$$

- **Effective pairing interaction *V*(*k*,*k'*) expanded to third order in *H'***

Linearized Eliashberg equation:

$$\lambda \cdot \Delta_{a\sigma_1\sigma_2}(k) = - \sum_{\substack{k',\sigma_3\sigma_4 \\ a'=\alpha,\beta,\gamma}} \underline{V_{a\sigma_1\sigma_2,a'\sigma_4\sigma_3}(k,k')}\, |G_{a'}(k')|^2 \, \Delta_{a'\sigma_3\sigma_4}(k')$$

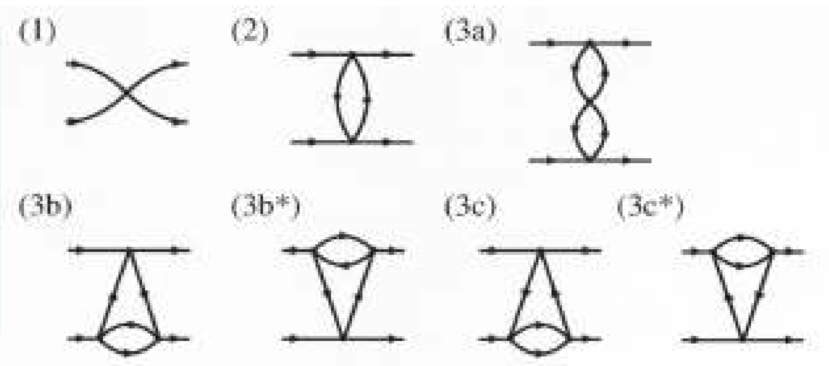

Superconducting order parameter: numerical solution of Eliashberg equation

$\Delta_{\alpha}(k), \Delta_{\beta}(k), \Delta_{\gamma}(k)$ **for the most probable pairing state:**

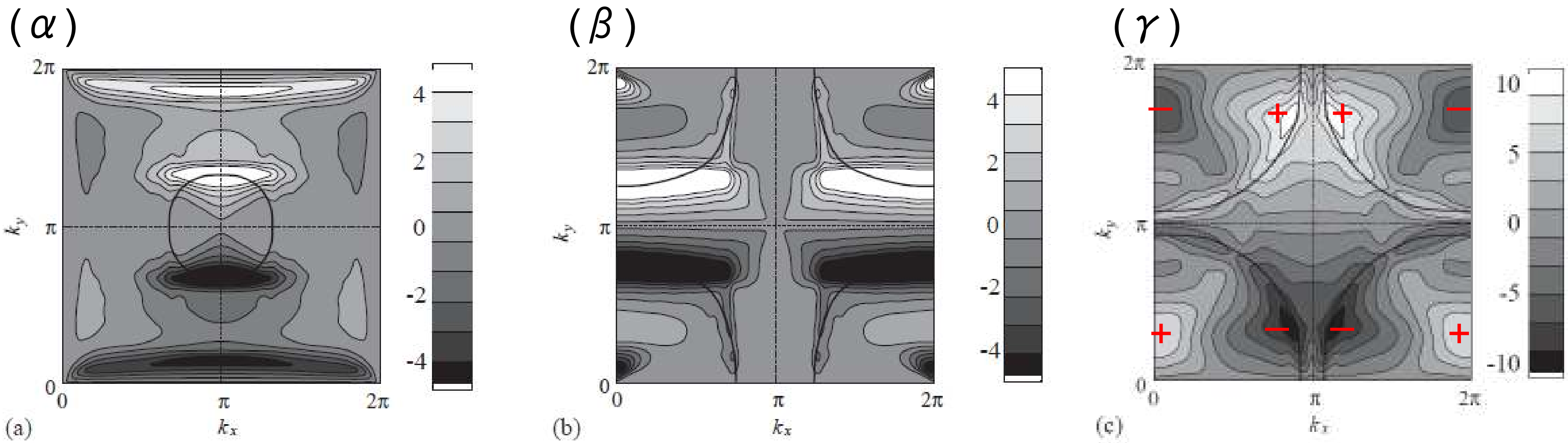

T. N. and K. Yamada, J. Phys. Soc. Jpn. 71, 1993 (2002).

- **Robust dominance of the γ band** (D.F. Agterberg et al. (1997)) .
  "Orbital Dependent Superconductivity"
- ***p*–wave-like on the γ band:**

$$\Delta_{\gamma}(k) \sim \sin k_y - 15.8 \times \cos k_x \sin k_y + \cdots$$

☺ R. P. Kaur et al. (2005),
" $\Delta(k) \sim \sin k_y - 12 \times \cos k_x \sin k_y$ "
explains the double transition in low-*T* and high-*H* region !

Superconducting gap structure in the chiral *p*-wave state

$$\Delta(\mathbf{k}) \sim f_x(\mathbf{k}) \pm i f_y(\mathbf{k})$$

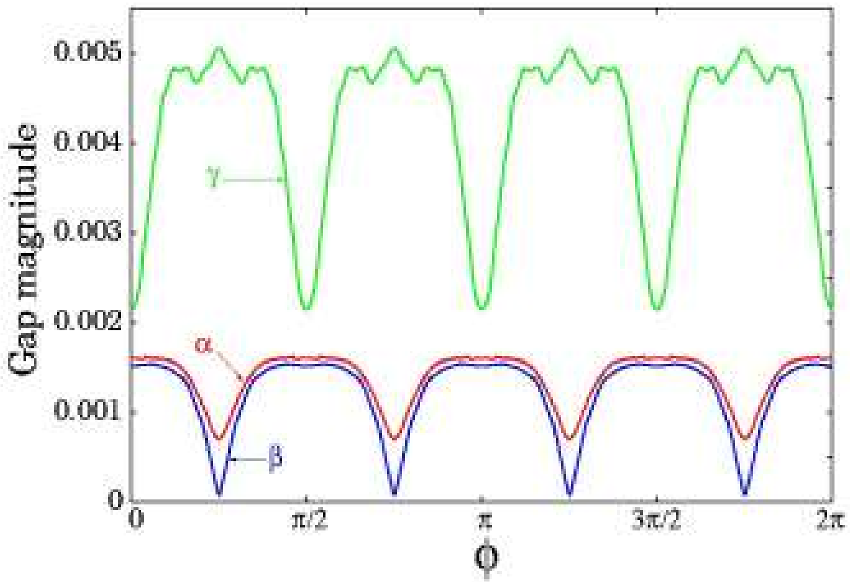

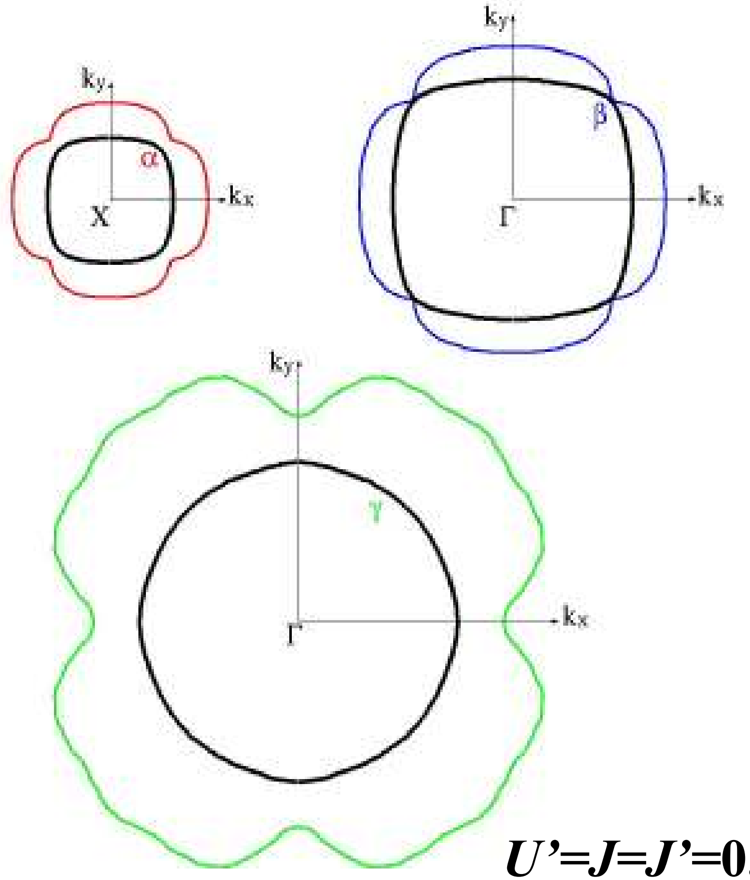

U'=J=J'=0.33U

- **There is a nodal structure on the γ band near the zone boundary.**
  ⇐ Odd-parity + 2π -periodicity in *k*-space (Miyake & Narikiyo (1999)).
- **There is a nodal structure on the α and β bands near the diagonal points.**
  ⇐ *p*-wave pairing attraction is suppressed there by the incommensurate fluctuation.

Specific heat

$$\Delta(\mathbf{k},T) \sim (f_x(\mathbf{k}) \pm i f_y(\mathbf{k}))\Delta(T)$$

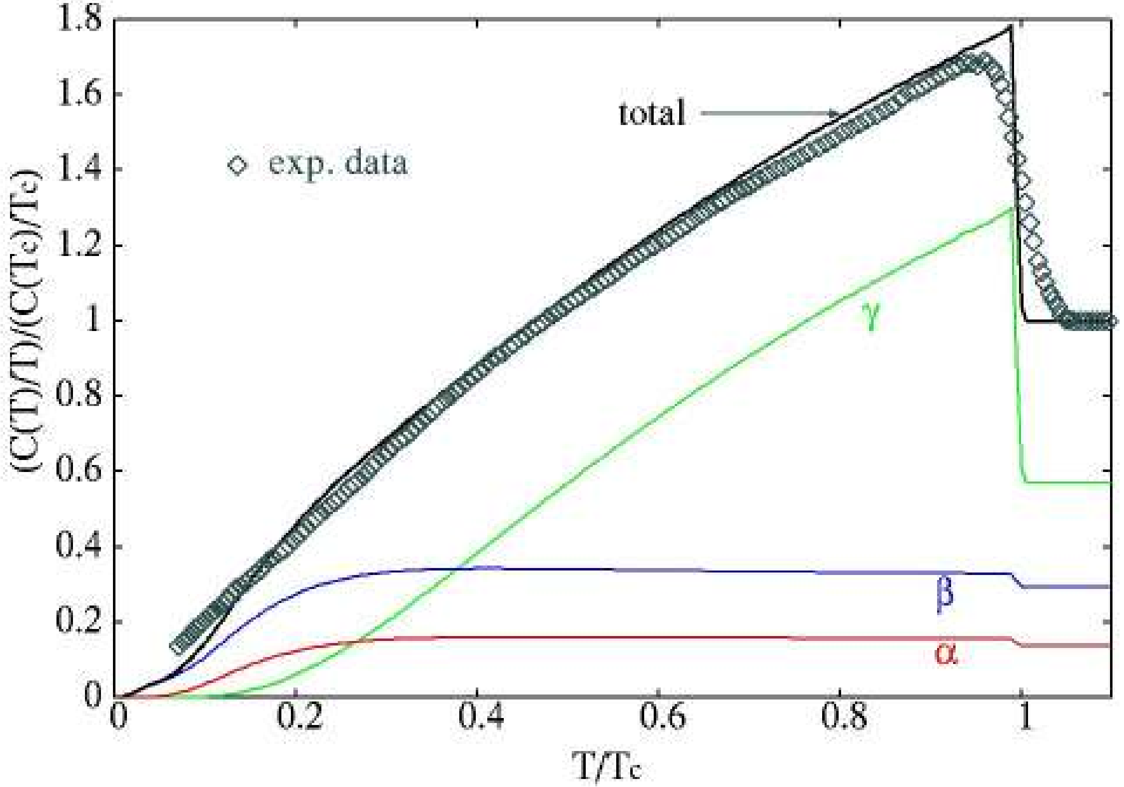

$$C = \sum_{\mathbf{k},a} E_a(\mathbf{k}) \frac{\partial f(E_a(\mathbf{k}))}{\partial T}$$

$$E_a(\mathbf{k}) = \sqrt{\xi_a(\mathbf{k})^2 + |\Delta_a(\mathbf{k},T)|^2}$$

U’=J=J’*=0.33*U

◇ : K. Deguchi, Y. Maeno, S. NishiZaki, et al.

T. Nomura & K. Yamada, J. Phys. Soc. Jpn. 71, 404 (2002).

◆ **The γ band dominates jump at *Tc*. At low *T*, the α and β bands are dominant.**

Ultrasound attenuation rate

Mean-Field Theory

T. N., J. Phys. Soc. Jpn. 74, 1818 (2005).

$$\Delta(\mathbf{k},T) \sim (f_x(\mathbf{k}) \pm i f_y(\mathbf{k}))\Delta(T)$$

◆ **The anisotropy of electron-phonon interaction is essential for explaining the strong in-plane anisotropy of ultrasound attenuation.**

(M.B. Walker, et al.)

⇒ **Fourier coefficients of electron-phonon coupling matrix are determined by fitting:**

$\tilde{g}_1 = 0.192$, $\tilde{g}_2 = 0.0096$, $\tilde{g}_3 = 0.0672$

$\tilde{g}_4 = 0.048$, $\tilde{g}_5 = 0.03072$

◆ **The γ band (active) is dominant for L100 mode, and the α, β bands (passive) are dominant for T100 mode.**

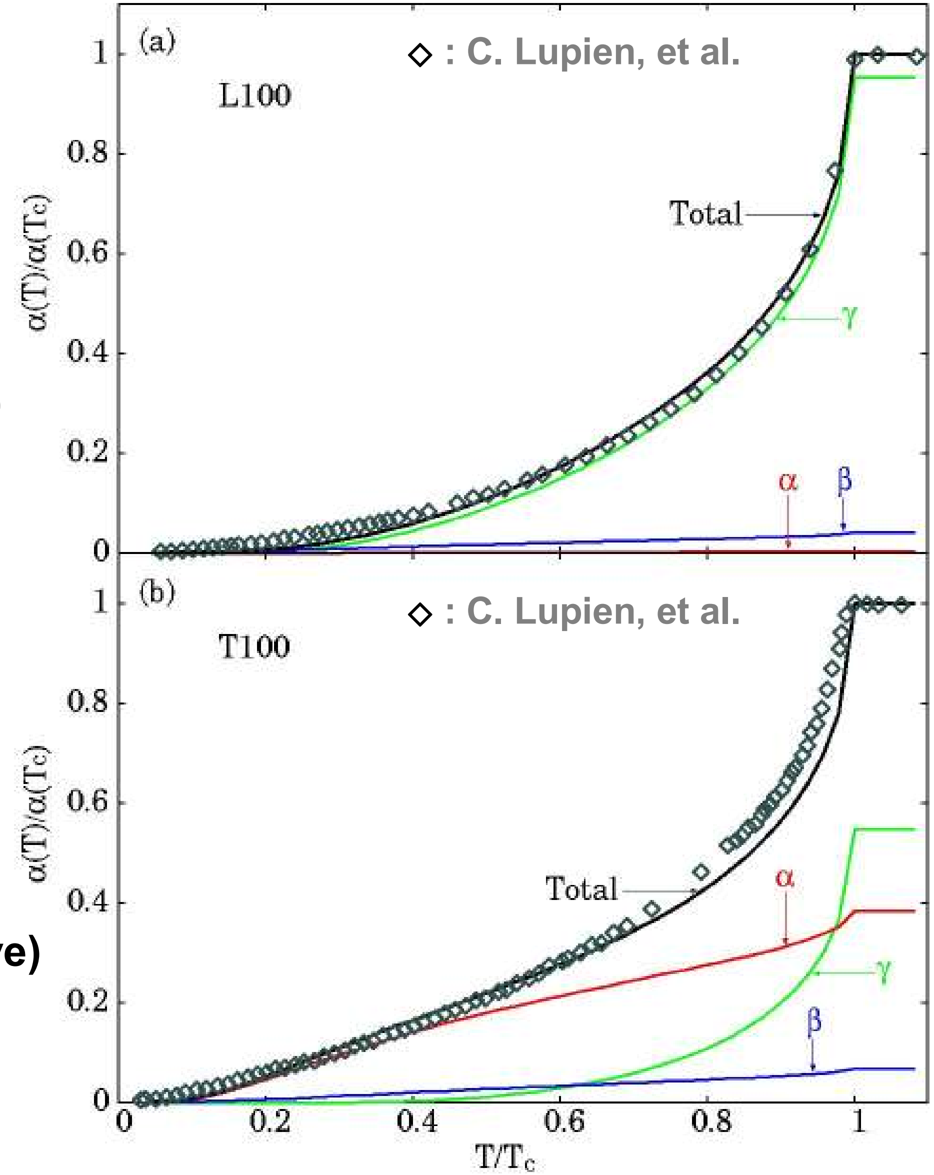

Thermal conductivity

Kubo Formula
+ Mean-Field Theory

$$\Delta(\mathbf{k},T) \sim (f_x(\mathbf{k}) \pm i f_y(\mathbf{k}))\Delta(T)$$

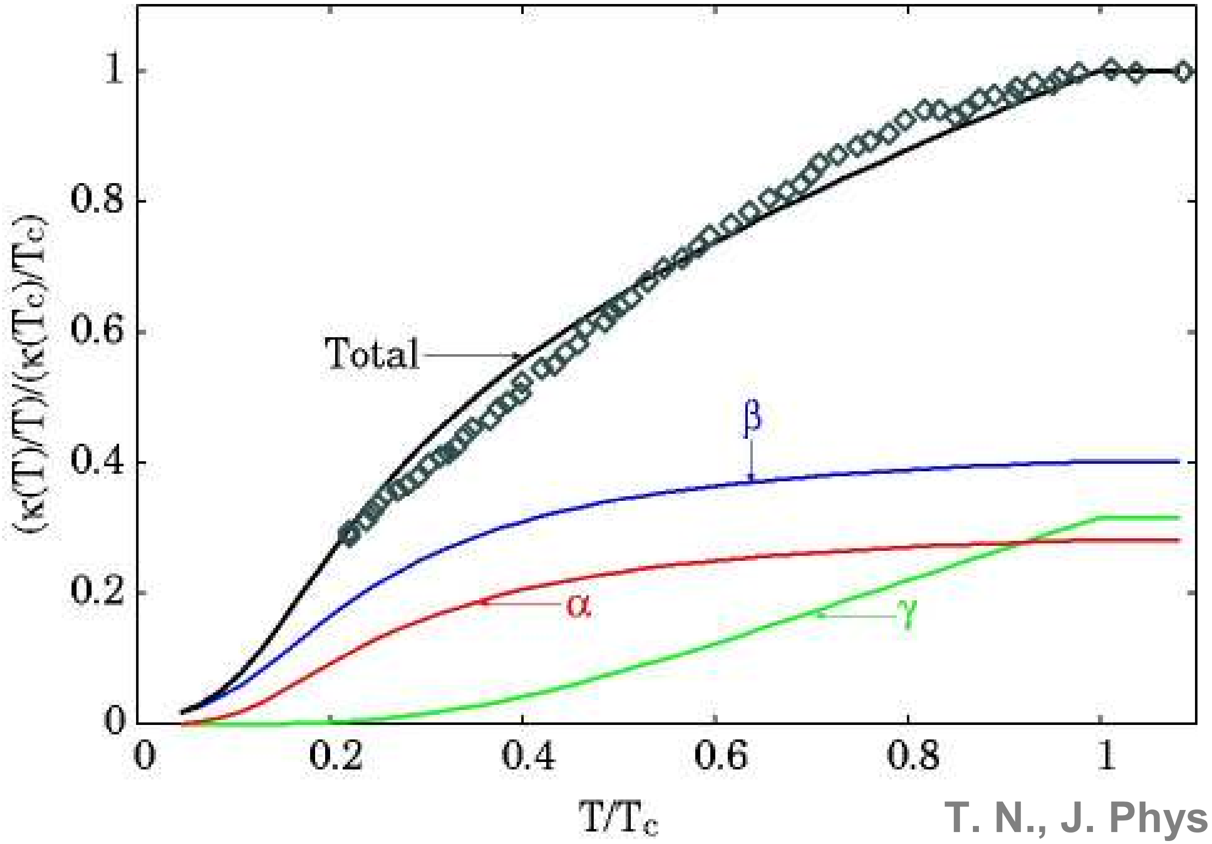

◇ : M. Tanatar et al.

T. N., J. Phys. Soc. Jpn. 74, 1818 (2005).

◆ The γ band does not effectively contribute to the thermal transport.
⇐ Fermi velocity is quite small at the nodal points
(i.e., near $(\pm\pi, 0)$, $(0, \pm\pi)$) on the γ Fermi surface.

NMR Relaxation rate

To appear in J. Phys. Chem. Solids.

$$\Delta(\mathbf{k},T) \sim (f_x(\mathbf{k}) \pm i f_y(\mathbf{k}))\Delta(T)$$

U_{RPA}=0.3U,
U'_{RPA}=0.3U',
J_{RPA}=0.3J.

U_{RPA}=0.3U,
U'_{RPA}=0.3U',
J_{RPA}=0.6J.

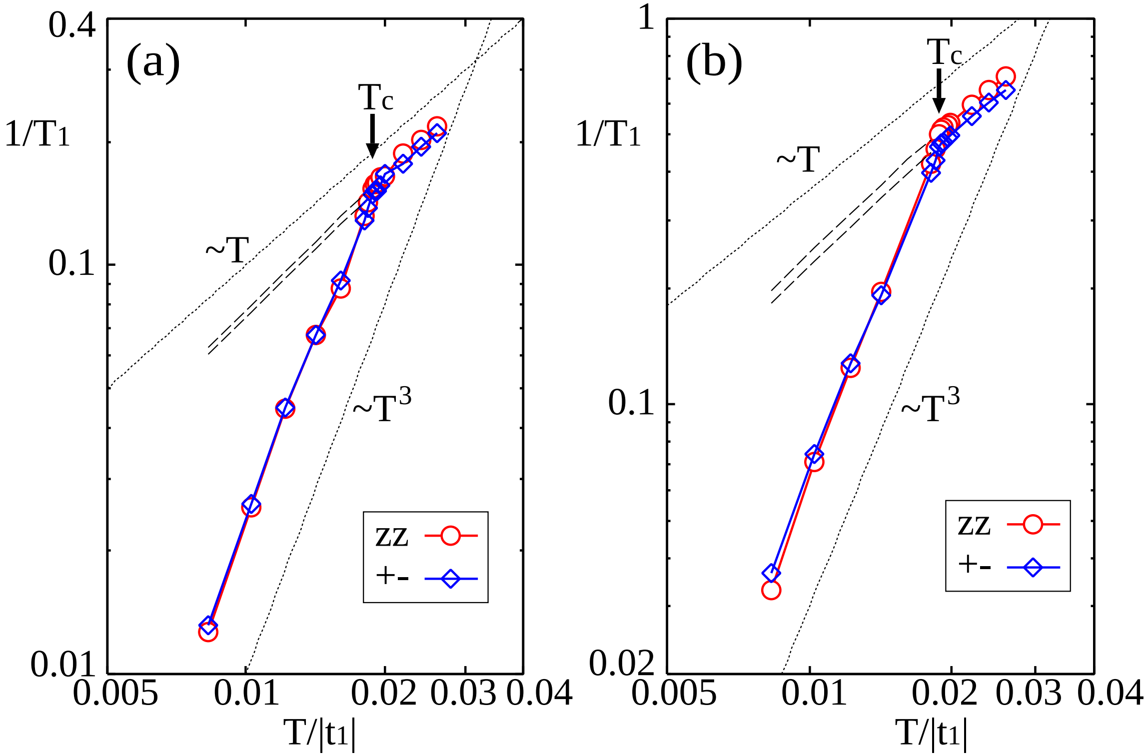

Experiment: K. Ishida et al.
PRL 84, 5387 (2000).

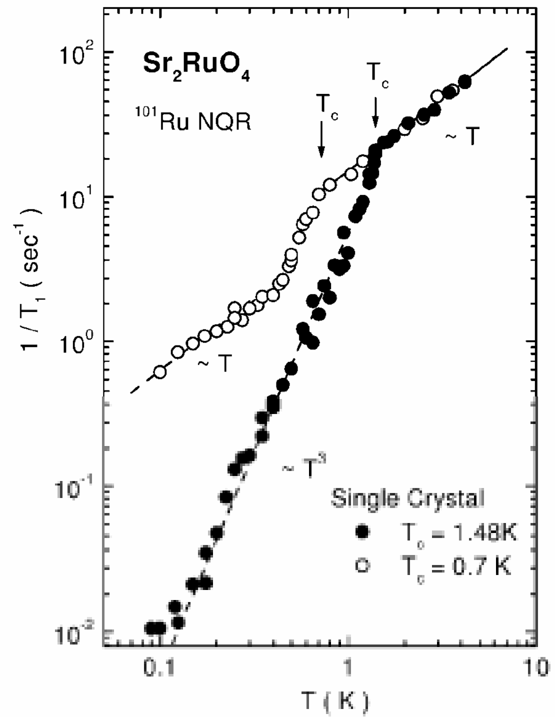

FIG. 1. T dependence of $1/T_1$ in low-T_c and high-T_c samples of Sr_2RuO_4.

- ◆ **Just below T_c, absence of Hebel-Slichter peak.**
- ◆ **For $T > T_c$, $1/T_1 \sim T$ (Korringa relation).**
- ◆ **For $T < T_c$, $1/T_1 \sim T^3$ (Line node-like behavior)**

Summary

The superconducting order parameter (gap function) could not be described only by one or a few harmonics. :

Approximately *$\sin k_x \cos k_y$*–wave like on the γ band, but more complex.

From the microscopic theory, the gap structure of Sr_2RuO_4 possesses large in-plane anisotropy and band dependence:

The γ band has the largest gap (active).
The gap minima on the γ band are located near $(\pm\pi,0)$ and $(0,\pm\pi)$.
The α,β bands have small gap (passive).
The gap minima (line-node-like) on the α,β bands are located near the diagonals.

The *T* dependences of specific heat, ultrasound attenuation rate, thermal conductivity and NMR relaxation rate *for the chiral state* are consistent with the experimental results at least in qualitative level.

Two transport coefficients: ultrasound attenuation rate and thermal conductivity

Ultrasound attenuation rate (in the hydrodynamic limit)

$$\alpha(T) = \frac{\omega_0(\mathbf{q})}{8T} \sum_{a,\mathbf{k}_\mathrm{F}} |\Lambda_{\mathbf{k}_\mathrm{F},\mathbf{q},a}|^2 \int_{-\infty}^{\infty} dz \frac{1}{\cosh^2[z/2T]} I_a(\mathbf{k}_\mathrm{F}, z)$$

Thermal conductivity tensor

Kubo Formula
+ Mean-Field Theory

$$\kappa_{\mu\nu}(T) = \frac{1}{8T^2} \sum_{a,\mathbf{k}_\mathrm{F}} v_{\mathbf{k}_\mathrm{F}a,\mu} v_{\mathbf{k}_\mathrm{F}a,\nu} \int_{-\infty}^{\infty} dz \frac{z^2}{\cosh^2[z/2T]} I_a(\mathbf{k}_\mathrm{F}, z)$$

using $I_a(\mathbf{k}_\mathrm{F}, z) = \left|\frac{\partial \xi_a(\mathbf{k})}{\partial \mathbf{k}}\right|_{\mathbf{k}=\mathbf{k}_\mathrm{F}}^{-1} \frac{1}{\mathrm{Im}\sqrt{\tilde{z}_a^\mathrm{R}(\mathbf{k}_\mathrm{F}, z)^2 - |\Delta_a(\mathbf{k}_\mathrm{F})|^2}} \left(1 + \frac{|\tilde{z}_a^\mathrm{R}(\mathbf{k}_\mathrm{F}, z)|^2 - |\Delta_a(\mathbf{k}_\mathrm{F})|^2}{\left|\tilde{z}_a^\mathrm{R}(\mathbf{k}_\mathrm{F}, z)^2 - |\Delta_a(\mathbf{k}_\mathrm{F})|^2\right|}\right)$

and $\tilde{z}_a^\mathrm{R}(\mathbf{k}_\mathrm{F}, z) = z - \Sigma_a^\mathrm{R}(\mathbf{k}_\mathrm{F}, z)$.

$\Sigma_a^\mathrm{R}(\mathbf{k}_\mathrm{F}, z)$ **is the self-energy due to non-magnetic impurity potential, and calculated by the self-consistent *T*-matrix approximation (in the unitarity limit).**

cf. P.J. Hirschfeld et al., S. Schmitt-Rink et al., for uranium compound superconductors.

Electron-phonon coupling matrix elements

Electron-phonon interaction

$$H_{\mathrm{ep}} = N^{-1/2} \sum_{\mathbf{kq},\ell\ell',\sigma} \Lambda_{\mathbf{k},\mathbf{q},\ell\ell'} (b_{\mathbf{q}} + b_{-\mathbf{q}}^{+}) c_{\mathbf{k}+\mathbf{q}\ell\sigma}^{+} c_{\mathbf{k}\ell'\sigma} \qquad \ell, \ell' = xy, yz, xz$$

Electron-phonon coupling matrix elements

$$\Lambda_{\mathbf{k},\mathbf{q},\ell\ell'} = i[2M\omega_0(\mathbf{q})]^{-1/2} \sum_{\mathbf{R}} e^{-i\mathbf{k}\cdot\mathbf{R}} [\mathbf{g}_{\ell\ell'}(\mathbf{R})\cdot\hat{\mathbf{e}}][\mathbf{q}\cdot\mathbf{R}]$$

Sum in *R* up to next nearest neighbors

$$\Lambda_{\mathbf{k},\mathbf{q},xy,xy} = i[\tilde{g}_1(\cos k_x \hat{e}_x \hat{q}_x + \cos k_y \hat{e}_y \hat{q}_y) + \tilde{g}_2 \cos k_x \cos k_y (\hat{e}_x \hat{q}_x + \hat{e}_y \hat{q}_y) - \tilde{g}_2 \sin k_x \sin k_y (\hat{e}_x \hat{q}_y + \hat{e}_y \hat{q}_x)]$$

$$\Lambda_{\mathbf{k},\mathbf{q},yz,yz} = i(\tilde{g}_4 \cos k_x \hat{e}_x \hat{q}_x + \tilde{g}_3 \cos k_y \hat{e}_y \hat{q}_y)$$

$$\Lambda_{\mathbf{k},\mathbf{q},xz,xz} = i(\tilde{g}_3 \cos k_x \hat{e}_x \hat{q}_x + \tilde{g}_4 \cos k_y \hat{e}_y \hat{q}_y)$$

$$\Lambda_{\mathbf{k},\mathbf{q},yz,xz} = \Lambda_{\mathbf{k},\mathbf{q},xz,yz} = i\tilde{g}_5[-\sin k_x \sin k_y (\hat{e}_x \hat{q}_x + \hat{e}_y \hat{q}_y) + \cos k_x \cos k_y (\hat{e}_x \hat{q}_y + \hat{e}_y \hat{q}_x)]$$

$$\Lambda_{\mathbf{k},\mathbf{q},\ell\ell'} = 0 \quad \text{(otherwise)}$$

The anisotropy of electron-phonon interaction is essential for explaining the strong in-plane anisotropy of ultrasound attenuation. ⇐ M.B. Walker, et al.

Ultrasound attenuation rate

Experimental Results of Viscosity (C. Lupien, et al.)

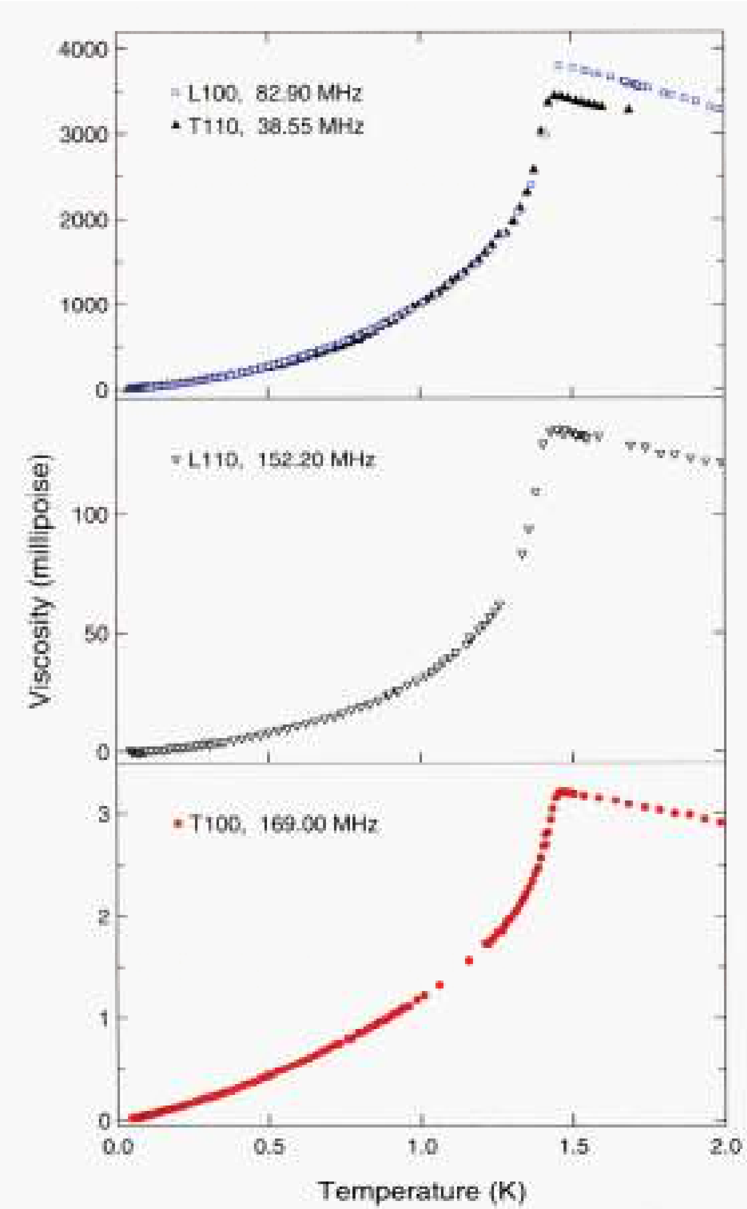

Theoretical Results of Sound Attenuation Rate

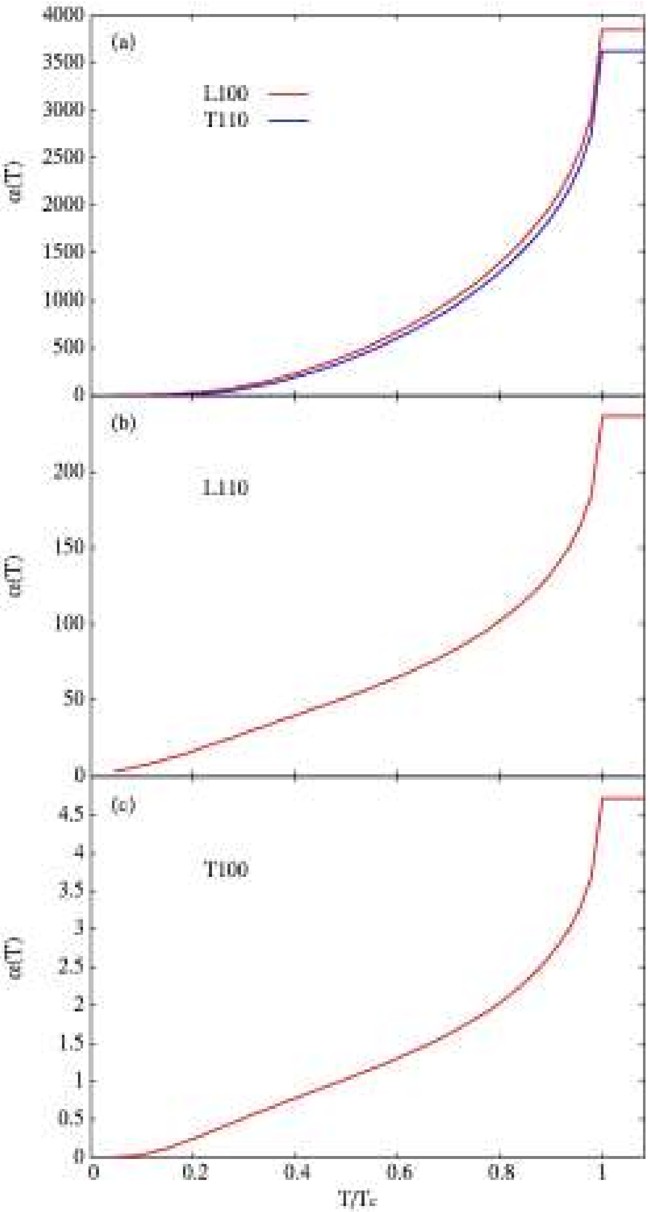

Density of states at *T*=0

$$\Delta(\mathbf{k},T) \sim (f_x(\mathbf{k}) \pm i f_y(\mathbf{k}))\Delta(T)$$